Simulation of Contaminants Transport in Groundwater From Nickel Mining Waste Dump Southeast Sulawesi

Kadek Nando Setiawan (kadeknandosetiawan00@gmail.com)
Universitas Pembangunan Nasional Veteran Yogyakarta https://orcid.org/0000-0002-8026-4588
Tedy Agung Cahyadi
Universitas Pembangunan Nasional Veteran Yogyakarta
Nur Ali Amri
Universitas Pembangunan Nasional Veteran Yogyakarta
Rika Ernawati
Universitas Pembangunan Nasional Veteran Yogyakarta
Nurkhamim Nurkhamim
Universitas Pembangunan Nasional Veteran Yogyakarta
Muhammad Iqbal Ansori
Universitas Pembangunan Nasional Veteran Yogyakarta
Ilham Firmansyah
Institut Teknologi Bandung
Sri Lastri Makarao
PT. Maha Bhakti Abadi

Research Article

Keywords: Groundwater, Numerical model, Solute transport, Nickel waste dump

Posted Date: January 7th, 2022

DOI: https://doi.org/10.21203/rs.3.rs-1122818/v1

Abstract

The irregularities of nickel resource mining in Indonesia cause many serious environmental problems. Piles of leftover rocks on nickel mining waste dumps have the potential to be a source of heavy metal seepage into the water. This study was conducted to assess the impact of nickel mining in the Langgikima Subdistrict of the North Konawe Regency of Southeast Sulawesi Province. The focus is to assess the migration of hexavalent chromium (Cr^{6+}) and iron (Fe) using MT3DMS to model the transport of solutes. The study's goal was to identify cr^{6+} and Fe concentrations in waste dumps and predict the spread of contaminants over a 20-year period of time. XRF (X-Ray Fluorescence) is done to determine the content of elements and minerals in rocks. Toxicity Characteristics Leaching Procedure (TCLP) is performed to estimate the concentration of Cr^{6+} and Fe in waste dumps. AAS (Atomic Absorption Spectrophotometer) to find out the content of Cr^{6+} and Fe in surface water and land water samples. The results showed the highest concentrations of Cr^{6+} of 0.0462 mg/L and Feat 0.8709 mg/L. Simulations without compacted clay coatings, Cr^{6+} and Fe contaminants could be transported consecutively by 2.7 km and 2.42 km while simulations used compacted clay layers with a hydraulic conductivity of 1×10^{-9} m/s of Cr^{6+} and Fe contaminants could be transported consecutively by 0.412 km and 0.467 km. It can therefore be concluded that heavy metals in the remaining rock piles from the waste dump can be transported into groundwater, and the action of using a compacted layer of clay must be taken to prevent contaminant migration into groundwater.

1. Introduction

Southeast Sulawesi province is an area in Indonesia with nickel reserves of 97.4 billion Wmt, spread over an area of 480 thousand hectares. This potential causes the number of mining companies in Southeast Sulawesi to grow rapidly, especially in recent years. The nickel mining system applied in Indonesia is an open-pit mine. The irregularities of nickel resource mining in Indonesia cause many serious environmental problems. Piles of leftover rocks in nickel mining waste dumps have the potential to be a source of heavy metal pollutants such as Pb, Cd, Cr, Fe, Cu, Zn, and Ni (Ngkoimani & Chaerul, 2017). Among these elements, cr has the strongest capacity to migrate under certain climatic conditions. Overburden containing high cr2O3 and Fe compounds can be a source of hexavalent chromium and iron seepage in surface water and groundwater (Tiwary et al., 2005).

Hexavalent chromium is soluble and highly mobile rather than the trivalent form. Cr^{6+} is highly carcinogenic and is known to be 100 – 1000 times more toxic than Cr^{3+} (trivalent chromium) (Linos et al., 2011). Cr^{6+} is known to cause cancer of the lungs, nasal cavity, paranasal sinuses, and stomach, as well as the larynx (Linos et al., 2011). Cr^{6+} is produced from the natural oxidation process of the cr^{3+} carrier mineral. Cr species are affected by pH and Eh water (Henderson, 1994). The release of Cr^{6+} into laterite groundwater is related to the oxidative reaction of Cr^{3+} with Mn oxide (Equeenuddin & Pattnaik, 2020; Fandeur et al., 2009), while the iron is a microelement that is essential for the body that is needed in the formation of blood, namely in hemoglobin (Hb), but if receiving too much Fe intake will cause various

health problems such as poisoning, where vomiting, diarrhea, intestinal damage, hemochromatosis, cirrhosis, liver cancer, diabetes, heart failure, arthritis, impotence, infertility, hypothyroidism, and chronic fatigue occurs (Agustina et al., 2021).

Analysis of dissolved Cr^{6+} content of liquid waste resulting from the remaining nickel mining of PT. Vale Tbk, found cr^{6+} concentration exceeded water quality standards (Marzuki, 2016). Water quality analysis results at nickel mines in New Caledonia show high concentrations of Cr^{6+} and are strongly affected by rainfall (Gunkel-Grillon et al., 2014). A study conducted by (Tiwary et al., 2018) in Sukinda Valley found high concentrations of Cr^{6+} in mine water (inlet mine water and outlet mine water), surface water, and groundwater. Then research (Okto et al., 2019) found high concentrations of Fe in river water around a nickel mining site in South Konawe, Southeast Sulawesi. Mine water with high concentrations of cr^{6+} and fe, which are not treated properly can be infallible into aquifers, leading to cr^{6+} and fe pollution in the land. (Dhakate et al., 2008; Tiwary et al., 2005) estimated the possibility of migration of Cr^{6+} into the aquifer using a transport model. (X. Wang et al., 2020) found cr^{6+} can diffuse vertically as deep as 58 m from ground level. Cr^{6+} contained in wastewater in eastern China can migrate 1,450 m within 10 years (Zhou et al., 2014).

Identifying the concentration of groundwater contaminant sources is essential for managing and protecting water from anthropogenic pressures (Soltani et al., 2017). Toxicity Characteristic Leaching Procedure (TCLP) is widely used to assess the concentration in waste (Adhikari & Mal, 2021; Lim et al., 2009; Sun et al., 2006; P. Wang et al., 2019). According to (Xie et al., 2021), many numerical simulation methods have been applied in the modeling of groundwater systems including FDM (Finite Difference Method), FEM (Finite Element Method), BEM (Boundary Element Method) and FAM (Finite Analytical Method). At this time with the development of data processing methods, Visual Modflow has been developed by Waterloo Hydrogeologic, Canada, which adopts different methods up to and combined with modern visualization technology. Visual Modflow software has the ability to simulate more complex conditions, can provide more realistic results, and is widely used to simulate groundwater flow, evaluate groundwater resources, and predict the spread of contaminants with MT3DMS packages (Adhikari & Mal, 2021; Ma et al., 2012; Rahman et al., 2018). Along with the development of technology, Visual Modflow can also be combined with a genetic algorithm (GA) in solving groundwater problems (Widodo et al., 2018). Identifying the concentration of groundwater contaminant sources is essential for managing and protecting groundwater from anthropogenic pressures (Soltani et al., 2017). Toxicity Characteristic Leaching Procedure (TCLP) is widely used to assess the concentration in waste (Adhikari & Mal, 2021; Lim et al., 2009; Sun et al., 2006; P. Wang et al., 2019). According to (Xie et al., 2021), many numerical simulation methods have been applied in the modeling of groundwater systems including FDM (Finite Difference Method), FEM (Finite Element Method), BEM (Boundary Element Method), and FAM (Finite Analytical Method). At this time with the development of data processing methods, Visual Modflow has been developed by Waterloo Hydrogeologic, Canada, which adopts different methods up to and combined with modern visualization technology. Visual Modflow software has the ability to simulate more complex conditions, can provide more realistic results, and is widely used to simulate groundwater

flow, evaluate groundwater resources, and predict the spread of contaminants with MT3DMS packages (Adhikari & Mal, 2021; Ma et al., 2012; Rahman et al., 2018). Along with the development of technology, Visual Modflow can also be combined with a genetic algorithm (GA) in solving groundwater problems (Widodo et al., 2018).

The aim of the study was to assess the concentrations of Cr^{6+} and Fe that can be escaped from leftover rocks in nickel mining waste dumps and conduct groundwater flow simulations using Visual Modflow as well as MT3DMS codes used to evaluate Cr^{6+} and Fe migrations in groundwater over 20 years across a variety of scenarios. This is the first time that water flow modeling and contaminant transport (Cr^{6+} and Fe) have been conducted at nickel mining areas in Southeast Sulawesi. The results of this study may have implications for planning the prevention or mitigation of groundwater pollution around nickel mining areas and provide input to the government on the determination of regulations in the design and layout of good waste dumps in nickel mining.

2. Study Area

The study area is located in the subwatershed of Langgikima Subdistrict, North Konawe Regency which covers an area of 56.25 km2 from 3°13'00" - 3°15'00" South Latitude and 122°14'2.8" - 122°17'10" East Longitude (Figure 1), where the Tobimeitta River flows northward while the Sari Mukti River flows westward. Average annual temperature – average 29.8° and average annual rainfall – averages 2404.9 mm. Waste dumps are located on the western part of the settlement with a general slope of high in the Southwest and low in the Northeast. The elevation is highest at 800 masl and the lowest is 25 masl. The slope in the west is quite steep, ranging from 25 - 49% and revolves from 0 - 2% in the East of the research area.

3. Material And Methods

3.1. Soil analysis in waste dump

Overburden (OB) is collected from nickel mining waste dumps as many as 5 samples and one soil sample is taken from settlements. Soil samples (about 1 kg each) are collected in HDPE plastic and used in geochemical studies and TCLP studies (Toxicity characteristic leaching procedures)

3.1.1. Characteristics of overburden

Geochemical studies include the characteristics of residential and overburdened soils in nickel mining waste dumps. Soil samples that have been collected are dried into an electric oven for ± 105°C, then ground into a dish mill machFluorescenceine for ± 8 minutes to the size of 200 mesh. Soil samples that have been finely tested XRF (X-Ray Fluorescence Spectroscopy) using epsilon 4 tools to find out the content of elements and minerals in the soil.

3.1.2. Toxicity characteristic leaching procedure (TCLP)

The TCLP study of the USEPA method (1990) was used to determine the potential for cr^{6+} and fe entangler in soil samples. Sodium acetate 1 M is used as an extraction fluid and the pH is maintained at 4.99. Then 100 grams of test samples are dissolved with 2 liters of extract solution according to the pH of the specified test sample. The solution is stored in a glass bottle and put into an extractor with a spin at 30 ± 2 rpm at a temperature of 25ºC for 18 hours. Then, the solution is filtered using Whatman class filter paper No. 42, the filter results are watered with HNO3 1: 6, then the metal is ready to be tested AAS (Atomic Absorption Spectrophotometer).

3.2. Hydrology Parameter

In groundwater modeling, it takes several important data that affect the result of models, one of which is a hydrological parameter. Hydrological parameters include evapotranspiration, run-off, and recharge. Calculation of evaporation of thornthwaite method (Seiler & Gat, 2007):

$$ET_r = \frac{p}{\sqrt{0{,}9 + \frac{p^2}{(300 + 25.Tm + 0{,}05.Tm^3)^2}}} \qquad (1)$$

Where, Etr is real evapotranspiration (mm/year); P is rainfall (mm/year); Tm is the average annual temperature (°C). Calculation of runoff water (run off) with empirical equations from the Indian Ministry of Agriculture (Haq et al., 2011):

$$R_o = \frac{1{,}511 \times p^{1{,}44}}{T_m^{1{,}34} \times A^{0{,}00618}} \qquad (2)$$

Where, Ro is run-off (cm/year); P is rainfall (mm/year); Tm is annual temperature (°C); A is watershed area (km2) Calculation of groundwater addition (recharge) using the Lerner formula in (Devy, 2019):

$$U = P - ET_r - Ro \qquad (3)$$

Where, U is the addition of groundwater (mm / year); P is rainfall (mm/year); ETr is real evapotranspiration (mm/year); Ro is run-off (mm/year). By applying the above equation, evapotranspiration, runoff, and appendages are calculated at 1,174, 331, and 899.23 mm/year, respectively.

3.3. Pemodelan airtanah

3.3.1. Mathematical groundwater flow model

Groundwater flow modeling uses Visual MODFLOW software. The program uses differential equations where structures are presented in grid form. By representing a different K value for each grid results in a K value distribution model similar to the fracture network in the field (Cahyadi et al., 2021). The partial differential equations that Visual Modflow software uses in heterogeneous and anisotropic porous media can be expressed as follows (Bair, 2016):

$$\frac{\partial}{\partial x}\left(-K_{xx}\frac{\partial h}{\partial x}\right)+\frac{\partial}{\partial y}\left(-K_{yy}\frac{\partial h}{\partial y}\right)+\frac{\partial}{\partial z}\left(-K_{zz}\frac{\partial h}{\partial z}\right)-W=S_s\frac{\partial h}{\partial t} \quad (4)$$

Where, Kxx, Kyy, Kzz is hydraulic conductivity in the direction of x, y and z (LT^{-1}); h is potential head (L); W is charging or pumping per unit area (LT^{-1}) Ss is specific storage (LT^{-1}) T is time (T).

3.3.2. Groundwater solute migration mathematical model

Transport of contaminants in groundwater is simulated using the CODE MT3DMS. In this model MT3DS is used to break down the transport of advection-dispersion contaminants from the groundwater flow model. Dissolved adsorption and chemical reactions of pollutants are not taken into account in this model given the complex reactions that may occur in the aquifer layer (Xie, 2021). Mathematical equations are used as follows:

$$\frac{\partial C}{\partial t}=\underbrace{\left[D_x\frac{\partial^2 C}{\partial x^2}+D_y\frac{\partial^2 C}{\partial y^2}+D_z\frac{\partial^2 C}{\partial z^2}\right]}_{\text{(dispertion)}}-\underbrace{\left[V_x\frac{\partial C}{\partial x}+V_y\frac{\partial C}{\partial y}+V_z\frac{\partial C}{\partial z}\right]}_{\text{(advection)}} \quad (5)$$

Where, C is the concentration of solution (M/L3); D is the dispersion coefficient (L2T); T is time (T); Vx is the average speed of linear groundwater (L/T).

3.3.3. Calibration model

After inputting data in groundwater modeling, it is continued with the model calibration, to match the calculated groundwater level with the measured. The value of groundwater recharge, boundary conditions, hydraulic parameters are adjusted within geological and hydrogeological limits. One of the criteria in matching the groundwater level is calculated and measured is by minimizing the value of RMS

(Root Mean Square) and NRMS (Normalized Root Mean Squared) to a minimum. RMS and NRMS values can be calculated by the equation:

$$RMS = \sqrt{\frac{1}{n}\sum_{i=1}^{n}(h_{obs} - h_{cal})_i^2} \quad (6)$$

$$NRMS(\%) = \frac{RMS}{\left(h_{obs}\right) max - (h_{0bs})\, min} \quad (7)$$

Where, n is the number of observation points; h_{obs} is the observed groundwater level; h_{cal} is the calculated result of groundwater level.

4. Result And Discussions

4.1. Soil analysis in waste dump

4.1.1. Waste dump characteristics

The heap of the covering layer is the main source of the release of toxic metals into the groundwater or surface water. This waste contains a percentage of certain elements and minerals that are the source of the release of toxic metals. Soils in the research area are laterite which contains a high percentage of iron oxide. The characteristics of samples of hoarded materials and residential soil are presented in Table 1. The results showed the content of Cr2O3 is about 2,409 - 2,985% and Fe about 44.58 - 49,183% in waste dump materials, which can be a source of hexavalent chromium and iron seepage in groundwater while the soil in settlements has a content of Cr2O3 2,949% and Fe 35,517%. Research areas in ophiolite rock formations cause high concentrations of Cr in soil, where cr concentrations range from 1800 mg/kg in ultramafic rocks (Kazakis et al., 2015).

Table 1
Results of analysis of elemental and mineral content in soil samples

NO	ID SAMPEL	ASSAY BY EPSILON 4						
		Ni (%)	Fe (%)	SIO2 (%)	MgO (%)	Co (%)	Al_2O_3 (%)	Cr_2O_3 (%)
1	TNH-1	1.204	49.001	2.27	1.737	0.114	6.417	2.792
2	TNH-2	1.138	44.734	2.614	1.681	0.118	8.986	2.8
3	TNH-3	1.097	44.58	2.376	2.003	0.116	8.835	2.659
4	TNH-4	0.984	47.438	1.52	1.334	0.103	9.551	2.409
5	TNH-5	1.149	49.183	1.693	1.134	0.119	7.012	2.985
6	TNH-6*	0.826	35.517	10.697	3.674	0.079	6.939	2.949
*) Samples outside the mine site								

4.1.2. Leachate characterization

A leachate study was conducted on two soil samples in the waste dump (TNH 2 and TNH 5) because it had the highest Cr2O3 content and one sample in the settlement. Results showed cr^{6+} and fe dissolved very low (Table 2). This is due to the fluid pH used in TCLP testing of 4.93 ± 0.05, which can increase the adsorption of chromate ions by oxides Mn, Fe, and Al (Gunkel-Grillon et al., 2014). At low pH, Cr^{6+} is absorbed by Mn oxide and can inhibit the release of Cr^{6+}, in addition, this can be attributed to the fact that with a decrease in pH, the activity of fe2+ ions becomes more facilitated reduction of Cr^{6+} to Cr^{3+} (Equeenuddin and Pattnaik, 2020). There are several factors that affect the release of metals in TCLP testing such as particle size, testing time, and pH.

Table 2
TCLP test results

Parameter	Satuan	Kode Sampel		
		TNH 2	TNH 5	TNH 6*
Fe	mg/l	0,01	0,003	0,022
Cr^{6+}	mg/l	< 0,006	< 0,006	< 0,006
*) Samples outside the mine site				

4.2. Surface and groundwater quality

Samplings of groundwater and surface water was conducted as many as 14 points, in May with average rainfall from 2009 - 2020 around 469 mm. Water quality testing results are presented in Table 3. Concentrations of Cr^{6+} in surface water ranged from 0.0235 – 0.0462 mg/L and Fe 0.6354 – 0.8709

mg/L, the highest concentrations of Cr^{6+} and Fe in surface water were found in sediment pond water samples (AP 2) of 0.0462 mg/L Cr^{6+} and 0.8709 Fe. The high concentration of Cr^{6+} is associated with the oxidation process of Cr^{3+} to Cr^{6+} (Equeenuddin & Pattnaik 2020). In water concentrations cr^{6+} ranged from 0.0223 – 0.0404 mg/L and Fe 0.1114 – 0.8606 mg/L, The highest concentration is in the sample of drill wells (ATB 2) in the mine which is 0.0404 mg / L Cr6 + and 0.8608 mg / L Fe which indicates there has been pollution, according to Dokou (Dokou et al., 2018) the concentration of Cr6 + in the natural condition in ultramafic rocks ranges from 0.02 mg / L so that the water sample in the drill well (ATB 2), Twice as much as its natural condition, while fe concentration has been 2.8 times greater than the standard quality of Class I with a threshold of 0.3 mg / L.

Table 3
Hasil analisis kualitas air

No	Kode Sampel	Koordinat		pH	Hasil Uji	
		X	Y		Cr^{6+} (mg/L)	Fe (mg/L)
1	ATB 1*	415671	9629952	7.2	0.0335	0.1342
2	ATB 2*	414802	9629022	7.15	0.0404	0.8608
3	ATP 1	414302	9632355	7.16	0.0265	0.6468
4	ATP 2	413980	9632201	7.2	0.0253	0.5165
5	ATP 3	413689	9632206	6.82	0.0249	0.1114
6	ATP 4	416015	9628848	6.73	0.0224	0.4886
7	ATP 5	415781	9628776	6.76	0.0246	0.5165
8	ATP 6	415824	9628807	6.82	0.0263	0.5481
9	ATP 7	416048	9628818	6.68	0.0299	0.6759
10	ATP 8	415989	9628571	6.73	0.0288	0.6595
11	ATP 9	416017	9628573	6.62	0.0223	0.4696
12	AP 1*	414929	9628300	7.15	0.0424	0.7759
13	AP 2*	414891	9628211	6.66	0.0462	0.8709
14	AP 3**	414579	9629650	6.8	0.0235	0.6354
* : Water samples in mine ATP : Water samples in settlement						
** : Water samples in river						

4.3. Hydrogeological conceptual model

Conceptual models are a simplification of complex field problems. Based on 52 drilling data, the research area rocks consist of weathering rocks (limonite and saprolite) and are based on ultramafic rocks. The limonite layer consists of clay and silt, which has a low permeability value so that it is considered an aquitard, saprolite layer is an aquifer in the research area consisting of a mixture of clay, silt, sand, gravel, and boulder, while ultramafic rock is the underlying layer of the model, the fracture part of this rock can pass water but with a small amount and is considered an aquitard. Based on hydrogeological conditions, aquifers of research areas include semi unconfined aquifers.

Hydraulic boundary conditions that limit the modeling area, namely the groundwater divide boundary, are in the western to southwestern mountainous areas that make the mountains as a no flow boundary, while the timut model is limited by the Tobimeitta river and the northern part of the model is limited by the Sari Mukti river, both rivers are used as river boundary. Recharge limit in the research area is obtained from the calculation of hydrological parameters which is 899.23 mm / year. Figure 2 is a conceptual model of groundwater flow.

4.4. Groundwater Modeling

To understand the flow patterns of groundwater in the research area, modeling is carried out using Visual Modflow software. The groundwater flow equation is solved by the code Modflow-2000 other methods up to those developed by USGS (Harbaugh et al., 2000) that can simulate the steady-state flow conditions of groundwater in form of 3 dimensions.

4.4.1. Model Discretization

The model was built with easting coordinate dimensions along 7.5 km and Northing along 7.5 km with a total area of 56.25 km2. The model is made using a horizontal grid size of 50 × 50 meters and divided into 3 layers in a vertical direction with a maximum elevation of 820 meters and a minimum of -80 meters. Details of the model grid design can be seen in Figure 3. Property input data is described in Table 4, which is obtained from various references. Because there has been no detailed hydrogeological study in the research area, aquifer property data is obtained from several literatures. The water system in the model is assumed to be a porous medium, which has homogeneous and isotropic properties in a horizontal direction (Kx = Ky), while in the vertical direction the hydraulic conductivity value is assumed to be less than 1 exponent order than the horizontal hydraulic conductivity value.

Table 4
Aquifer properties of the research area

Hydraulic Parameter	Geological Unit			References
	Clay-Silt	Fine sand-Boulder	Ultramafic Rock	
Hydraulic Conductivity (m/s)	$1,4 \times 10^{-7}$	5×10^{-6}	5×10^{-8}	Freeze and Cherry (1979), Splitz & Moreno (1996)
Specific Storage (1/m)	1×10^{-2}	3×10^{-2}	1×10^{-4}	Domenico & Mifflin, 1965
Specific Yield (%)	15	22.6	12	Heath (1983)
Effective Porosity (%)	15	33	10	McWorter and Sunada (1977)
Total Porosity (%)	40	35	11	Heath (1983), Freeze and Cherry (1979)

4.4.2. Flow model calibration

The calibration model aims to produce the groundwater level and the direction of the water flow in accordance with field conditions (Surinaidu et al., 2014). Calibration of the groundwater flow model is achieved through the trial and error method by adjusting two main parameters, namely hydraulic conductivity and recharge. The 11 wells measured in May 2021 were used in the calibration process. The results of the model calibration showed a correlation coefficient value of 0.975 m, an RMS value of 2,918 m, and an NRMS value of 7.044%, and a residual mean of -0.145 m. These results are considered to be close to the actual conditions of the field. Calibration of the flow model can be seen in Figure 4.

Sensitivity analysis is conducted to evaluate uncertainties associated with model input parameters (Peksezer-Sayit et al., 2015; Xue et al., 2018). Hydraulic conductivity and recharge parameters are varied by multiplying the values of calibrated parameters by some coefficients shown on the horizontal axis, then comparing the RMSE values at the end of each simulation. The sensitivity analysis can be seen in Figure 4. The results of the sensitivity plot showed that the model was most sensitive to the decrease in hydraulic conductivity in ultramafic rocks, while in the sensitivity analysis of recharge parameters, the model was most sensitive to the addition of recharge values

4.5. Contaminant transport modeling

The model parameters used in the simulation of contaminant transport of steady-state conditions are the parameters of the groundwater flow model that have been calibrated. Additional constant concentration parameters are used to simulate pollution in nickel mine waste dumps. Constant concentration is inputted as wide as the waste dump area placed on layer 1. The initial concentration used in the model is

the concentration of Cr^{6+} and Fe test results on 9 resident wells. The MT3DMS module is run to model contaminant transport.

4.5.1. Contaminant model calibration

In this modeling, we try to calibrate the contaminant transport model. The purpose of calibration of the contaminant transport model is to match the concentration of the calculation results with the concentration of field measurement results (Dokou et al., 2018; Rao et al., 2011; Xie et al., 2021; Chen et al., 2016). The calibration model shows the concentration of Cr^{6+} and Fe contaminants close to field conditions (Figure 6), with RMS values of 0.05 mg/L, NRMS of 7.839% and correlation coefficients of 0.985 so that the model can be used to predict the transport of contaminants in transient conditions.

4.5.2. Model Application

Calibrated contaminant models are used to predict the spread of Cr^{6+} and Fe contaminants in two scenarios: Scenario-A (without a compacted layer of clay on a waste dump base) and Scenario-B (using a compacted clay layer on a waste dump basis). To study the effect of compacted clay layers on groundwater quality, we made a model of adding a compacted clay layer with a permeability coefficient of 1×10^{-9} m / s and a depth of 10 cm. The simulation time is set at 20 years and the output time specified is 1, 5, 10, and 20 years, respectively.

The results of simulations of Cr^{6+} and Fe in 2 scenarios at the aquifer layer are shown in (Figure 7 and Figure 8). Seen from Figure 7(a) and Figure 8(a) is a simulation of Scenario-A, contaminants move following the flow pattern of groundwater from the West polluting source (waste dump) to the East model that shows the influence of the advection process (Datta et al., 2017). The range of plume migration in 0 - 5 years is faster than in 10 - 20 years. Therefore, with the expansion of the migration range, the plume diffusion rate gradually slows down (Xie et al., 2021). In the first year, the concentration of Cr^{6+} was 0.0316 mg/L and Fe was 0.6411 mg/L at polluting sources, with migration distances of 0.324 km for Cr^{6+} and 0.315 km for Fe. In the 5th year, the concentration of Cr^{6+} was 0.0436 mg/L and Fe was 0.8304 mg/L at polluter sources, with a migration distance of 1.24 km for Cr^{6+} and 1.21 km for Fe. In the 10th year, the concentration of Cr^{6+} was 0.0437 mg/L and Fe was 0.8311 mg/L at polluting sources, with a migration distance of 2.25 km for Cr^{6+} and 2.14 km for Fe. In the 20th year, cr^{6+} concentrations were 0.0436 mg/L and Fe was 0.83 mg/L at polluting sources, with migration distances of 2.7 km for Cr^{6+} and 2.42 km for Fe. The average speed of cr^{6+} spread is about 135 m/year while Fe is about 121 m/year. The concentration of Cr^{6+} is still below the class I water quality standard of 0.05 mg / L, while the fe concentration has exceeded the class I quality standard of 0.3 mg / L.

Figure 7(b) and Figure 8(b) show the results of scenario-B simulations, where there is a significant difference in the distance of the plume spread with Scenario-A. Cr^{6+} spread distance in the 20th year is 0.412 km with an average speed of 20.6 m / year, while the spread distance of Fe in the 20th year is

0.467 km with an average speed of 23.35 m / year. From these results, it is proven that the addition of a compacted clay layer on the basis of the waste dump can suppress the plume spread distance. This is because the value of hydraulic conductivity plays a big role in reducing the distance of plume distribution in contaminant transport that only takes into account the advection-dispersion process (Torres, 2020). But the Concentration of Cr^{6+} of 0.038 mg / L and Fe of 0.75 mg / L was found in the Observation well 1 which is 50 m away from the waste dump in the 20th year, which shows plume can still penetrate the compacted clay layer, it is also due to the thin aquifer layer that ranges from 3- 28 m so that in modeling the aquifer layer is quickly saturated with contaminants. Plume migration in Scenario-B did not reach the Observation 3 well which is 500 meters from the waste dump in the 20th year of the simulation.

5. Conclusions

Numerical simulations were used to model the flow and transport of contaminants at nickel mine sites. Model calibration is used to find optimal parameters and minimize computer calculation errors with field survey data so as to help us in predicting contaminant transport over the next 20 years. The results of TCLP testing showed cr^{6+} and fe that can be separated from waste rocks in the waste dump are so small that the concentration of pollutant sources used is the result of testing water samples in sediment ponds that accommodate leaching results from waste dumps with the content of Cr^{6+} 0.0462 mg / L which is still below the Class I quality standard while fe content has exceeded the Class I quality standard of 0.8709 mg / L.

The results of MT3DMS simulation for 20 years, revealed that Cr^{6+} and Fe can migrate rapidly in the aquifer layer, but when the addition of a safety layer in the form of a compacted clay layer on the basis of a waste dump that has a conductivity value of 1×10^{-9} m / s, resulting in the distance and speed of plume spread is shorter even the spread distance is not up to 500 meters from the waste dump and plume has not passed the mine boundary in the 20th year simulation, So as to create sustainable exploitation of mining resources in accordance with the conservation of southeast Sulawesi's natural environment, the author strongly encourages the mining industry to use a compacted clay layer at the base of the waste dump and pay attention to the layout and distance of waste dumps with settlements. z

References

1. Adhikari, K., & Mal, U. (2021). Evaluation of contamination of manganese in groundwater from overburden dumps of Lower Gondwana coal mines. *Environmental Earth Sciences*, *80*(1), 1–15. https://doi.org/10.1007/s12665-020-09293-9
2. Agustina, N., Aquarista, M. F., Masyarakat, F. K., Islam, U., Uniska, K., & Banjarmasin, M. A. B. (2021). *Kualitas Air Rawa terhadap Keluhan Kesehatan Masyarakat Desa The Quality of Water Swamp on Complaints Health Villagers*. *12*, 220–227.
3. Bair, E. S. (2016). Applied Groundwater Modeling-Simulation of Flow and Advective Transport. In *Groundwater* (Vol. 54, Issue 6). https://doi.org/10.1111/gwat.12464

4. Cahyadi, T. A., Syihab, Z., Widodo, L. E., Notosiswoyo, S., & Widijanto, E. (2021). Analysis of hydraulic conductivity of fractured groundwater flow media using artificial neural network back propagation. *Neural Computing and Applications*, *33*(1), 159–179. https://doi.org/10.1007/s00521-020-04970-z
5. Chen, C. S., Tu, C. H., Chen, S. J., & Chen, C. C. (2016). Simulation of groundwater contaminant transport at a decommissioned landfill site—A case study, Tainan City, Taiwan. In *International Journal of Environmental Research and Public Health* (Vol. 13, Issue 5). https://doi.org/10.3390/ijerph13050467
6. Datta, B., Petit, C., Palliser, M., Esfahani, H. K., & Prakash, O. (2017). Linking a Simulated Annealing Based Optimization Model with PHT3D Simulation Model for Chemically Reactive Transport Processes to Optimally Characterize Unknown Contaminant Sources in a Former Mine Site in Australia. *Journal of Water Resource and Protection*, *09*(05), 432–454. https://doi.org/10.4236/jwarp.2017.95028
7. Devy, S. D. (2019). Pemodelan airtanah dan Neraca Airtanah Dampak Penambangan Batubara Open Pit pada Lipatan Sinklin di Daerah Muara Lawa, Kabupaten Kutai Barat, Provinsi Kalimantan Timur. *SPECTA Journal of Technology*, *2*(2), 69–83. https://doi.org/10.35718/specta.v2i2.108
8. Dhakate, R., Singh, V. S., & Hodlur, G. K. (2008). Impact assessment of chromite mining on groundwater through simulation modeling study in Sukinda chromite mining area, Orissa, India. *Journal of Hazardous Materials*, *160*(2–3), 535–547. https://doi.org/10.1016/j.jhazmat.2008.03.053
9. Dokou, Z., Karatzas, G. P., Nikolaidis, N. P., & Kalogerakis, N. (2018). *Modeling the Groundwater Flow and Hexavalent Chromium Transport in the Asopos River Basin*. *September*.
10. Equeenuddin, S. M., & Pattnaik, B. K. (2020). Hydrogeochemical evolution of hexavalent chromium at the Sukinda ultramafic complex in eastern part of India. *Chemie Der Erde*, *80*(4), 125633. https://doi.org/10.1016/j.chemer.2020.125633
11. Fandeur, D., Juillot, F., Morin, G., Livi, L., Cognigni, A., Webb, S. M., Ambrosi, J. P., Fritsch, E., Guyot, F., & Brown, G. E. (2009). XANES evidence for oxidation of Cr(III) to Cr(VI) by Mn-oxides in a lateritic regolith developed on serpentinized ultramafic rocks of New Caledonia. *Environmental Science and Technology*, *43*(19), 7384–7390. https://doi.org/10.1021/es900498r
12. Gunkel-Grillon, P., Laporte-Magoni, C., Lemestre, M., & Bazire, N. (2014). Toxic chromium release from nickel mining sediments in surface waters, New Caledonia. *Environmental Chemistry Letters*, *12*(4), 511–516. https://doi.org/10.1007/s10311-014-0475-1
13. Haq, S., Prakasa, D., Putra, E., Hendrayana, H., & Igarashi, T. (2011). Hydrogeology of an Open-pit Coal Mine in Tamiang Layang, Central Kalimantan, Indonesia: a Preliminary Groundwater Flow Modeling. *Indonesian Association Geologists (IAGI)*, *July*, 1–20.
14. Henderson, T. (1994). Geochemical Reduction of Hexavalent Chromium in the Trinity Sand Aquifer. *Groundwater*, *32*(3), 477–486. https://doi.org/10.1111/j.1745-6584.1994.tb00665.x
15. Kazakis, N., Kantiranis, N., Voudouris, K. S., Mitrakas, M., Kaprara, E., & Pavlou, A. (2015). Geogenic Cr oxidation on the surface of mafic minerals and the hydrogeological conditions influencing

hexavalent chromium concentrations in groundwater. *Science of the Total Environment*, *514*, 224–238. https://doi.org/10.1016/j.scitotenv.2015.01.080

16. Lim, M., Han, G. C., Ahn, J. W., You, K. S., & Kim, H. S. (2009). Leachability of arsenic and heavy metals from mine tailings of abandoned metal mines. *International Journal of Environmental Research and Public Health*, *6*(11). https://doi.org/10.3390/ijerph6112865
17. Linos, A., Petralias, A., Christophi, C. A., Christoforidou, E., Kouroutou, P., Stoltidis, M., Veloudaki, A., Tzala, E., Makris, K. C., & Karagas, M. R. (2011). Oral ingestion of hexavalent chromium through drinking water and cancer mortality in an industrial area of Greece - An ecological study. *Environmental Health: A Global Access Science Source*, *10*(1), 1–8. https://doi.org/10.1186/1476-069X-10-50
18. Ma, C. A., Li, K. M., & Zhao, S. P. (2012). Study on the solute transport modeling of opencast mine groundwater. *Advanced Materials Research*, *356–360*, 1699–1703. https://doi.org/10.4028/www.scientific.net/AMR.356-360.1699
19. Marzuki, I. (2016). Analisis Chromium Hexavalent dan Nikel Terlarut dalam Limbah Cair Area Pertambangan PT VALE Tbk . Soroako-Indonesia Analysis of Hexavalent Chromium and Dissolved Nickel in Water Waste Used in Mining Area of PT VALE Tbk . Soroako-Indonesia. *Jurnal Chemica*, *17*(2), 1–11.
20. Ngkoimani, L. O., & Chaerul, M. (2017). *Impacts of Nickel Laterite Post-Mining Activities on The Level of Heavy Metal Contamination in River Sediments*. *149*(Icest), 240–242. https://doi.org/10.2991/icest-17.2017.78
21. Okto, A., Ngkoimani, L. O., Asfar, A., Jahiddin, Firman, A., & Marwan. (2019). Analisis Pengaruh Aktivitas Pertambangan Terhadap Kualitas Air Tanah Di Kabupaten Konawe Selatan. *Jurnal Geologi Terapan*, *01*(Cd), 43–52.
22. Peksezer-Sayit, A., Cankara-Kadioglu, C., & Yazicigil, H. (2015). Einschätzung der benötigten Entwässerung und der erwarteten Auswirkungen auf Grundwasservorräte: Eine Fallstudie über den Caldag Nickelbergbau, westliche Türkei. *Mine Water and the Environment*, *34*(2), 122–135. https://doi.org/10.1007/s10230-014-0306-4
23. Rahman, H. A., Putra, D. P. E., & Hendrayana, H. (2018). Pemodelan Pergerakan Pencemar Airtanah oleh Hidrokarbon di Kelurahan Jlagran Kota Yogyakarta. *Jurnal Geosains Dan Teknologi*, *1*(3), 81. https://doi.org/10.14710/jgt.1.3.2018.81-88
24. Rao, G. T., Rao, V. V. S. G., Ranganathan, K., Surinaidu, L., Mahesh, J., & Ramesh, G. (2011). Assessment of groundwater contamination from a hazardous dump site in Ranipet, Tamil Nadu, India. *Hydrogeology Journal*, *19*(8), 1587–1598. https://doi.org/10.1007/s10040-011-0771-9
25. Soltani, S., Asghari Moghaddam, A., Barzegar, R., Kazemian, N., & Tziritis, E. (2017). Hydrogeochemistry and water quality of the Kordkandi-Duzduzan plain, NW Iran: application of multivariate statistical analysis and PoS index. *Environmental Monitoring and Assessment*, *189*(9). https://doi.org/10.1007/s10661-017-6171-4

26. Sun, Y., Xie, Z., Li, J., Xu, J., Chen, Z., & Naidu, R. (2006). Assessment of toxicity of heavy metal contaminated soils by the toxicity characteristic leaching procedure. *Environmental Geochemistry and Health*, *28*(1–2). https://doi.org/10.1007/s10653-005-9014-0
27. Surinaidu, L., Gurunadha Rao, V. V. S., Srinivasa Rao, N., & Srinu, S. (2014). Hydrogeological and groundwater modeling studies to estimate the groundwater inflows into the coal Mines at different mine development stages using MODFLOW, Andhra Pradesh, India. *Water Resources and Industry*, *7–8*, 49–65. https://doi.org/10.1016/j.wri.2014.10.002
28. Tiwary, R. K., Dhakate, R., Ananda Rao, V., & Singh, V. S. (2005). Assessment and prediction of contaminant migration in ground water from chromite waste dump. *Environmental Geology*, *48*(4–5), 420–429. https://doi.org/10.1007/s00254-005-1233-2
29. Tiwary, R. K., Kumari, B., & Singh, D. B. (2018). *Water Quality Assessment and Correlation Study of Physico-Chemical Parameters of Sukinda Chromite Mining Area, Odisha, India*. 357–370. https://doi.org/10.1007/978^{-9}81-10-5792-2_29
30. Torres, H. (2020). Assessing Groundwater Contamination Risk and Detection of Unknown Sources Using a Multi-Component Reactive Transport Model. *Journal of Geoscience and Environment Protection*, *08*(05), 132–158. https://doi.org/10.4236/gep.2020.85009
31. Wang, P., Sun, Z., Hu, Y., & Cheng, H. (2019). Leaching of heavy metals from abandoned mine tailings brought by precipitation and the associated environmental impact. *Science of the Total Environment*, *695*. https://doi.org/10.1016/j.scitotenv.2019.133893
32. Wang, X., Li, L., Yan, X., Meng, X., & Chen, Y. (2020). Processes of chromium (VI) migration and transformation in chromate production site: A case study from the middle of China. *Chemosphere*, *257*, 127282. https://doi.org/10.1016/j.chemosphere.2020.127282
33. Widodo, L. E., Cahyadi, T. A., Syihab, Z., Notosiswoyo, S., Iskandar, I., & Rustamaji, H. C. (2018). Development of drain hole design optimisation: a conceptual model for open pit mine slope drainage system with fractured media using a multi-stage genetic algorithm. *Environmental Earth Sciences*, *77*(20), 0. https://doi.org/10.1007/s12665-018-7895-3
34. Xie, W., Ren, B., Hursthouse, A. S., Wang, Z., & Luo, X. (2021). Simulation of manganese transport in groundwater using visual modflow: A case study from xiangtan manganese ore area in central china. *Polish Journal of Environmental Studies*, *30*(2), 1409–1420. https://doi.org/10.15244/pjoes/125766
35. Xue, S., Liu, Y., Liu, S., Li, W., Wu, Y., & Pei, Y. (2018). Numerical simulation for groundwater distribution after mining in Zhuanlongwan mining area based on visual MODFLOW. *Environmental Earth Sciences*, *77*(11), 0. https://doi.org/10.1007/s12665-018-7575-3
36. Zhou, Y., Jiang, Y., An, D., Ma, Z., Xi, B., Yang, Y., Li, M., Hao, F., & Lian, X. (2014). Simulation on forecast and control for groundwater contamination of hazardous waste landfill. *Environmental Earth Sciences*, *72*(10), 4097–4104. https://doi.org/10.1007/s12665-014-3302-x

Figures

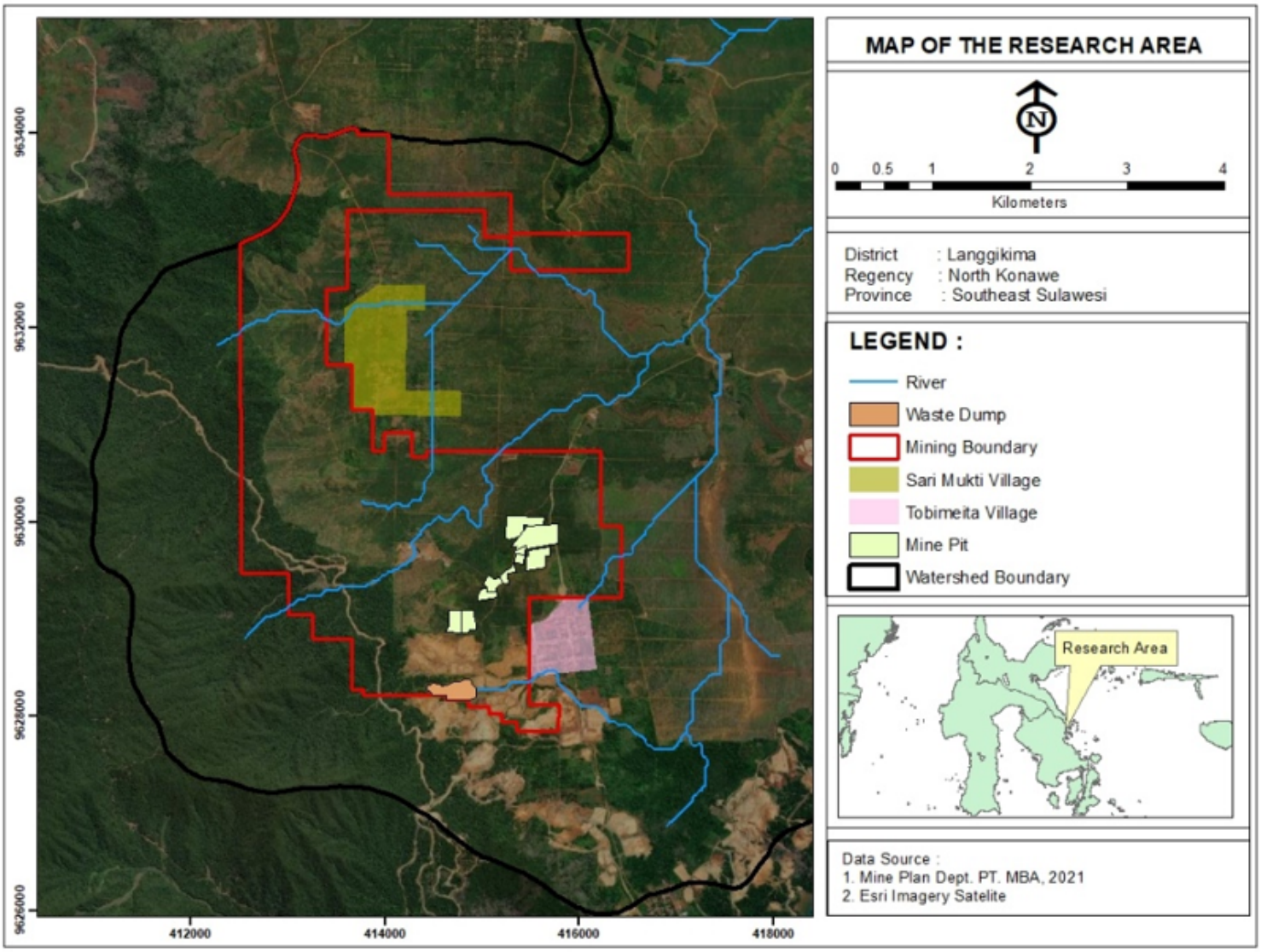

Figure 1

Map of the research area

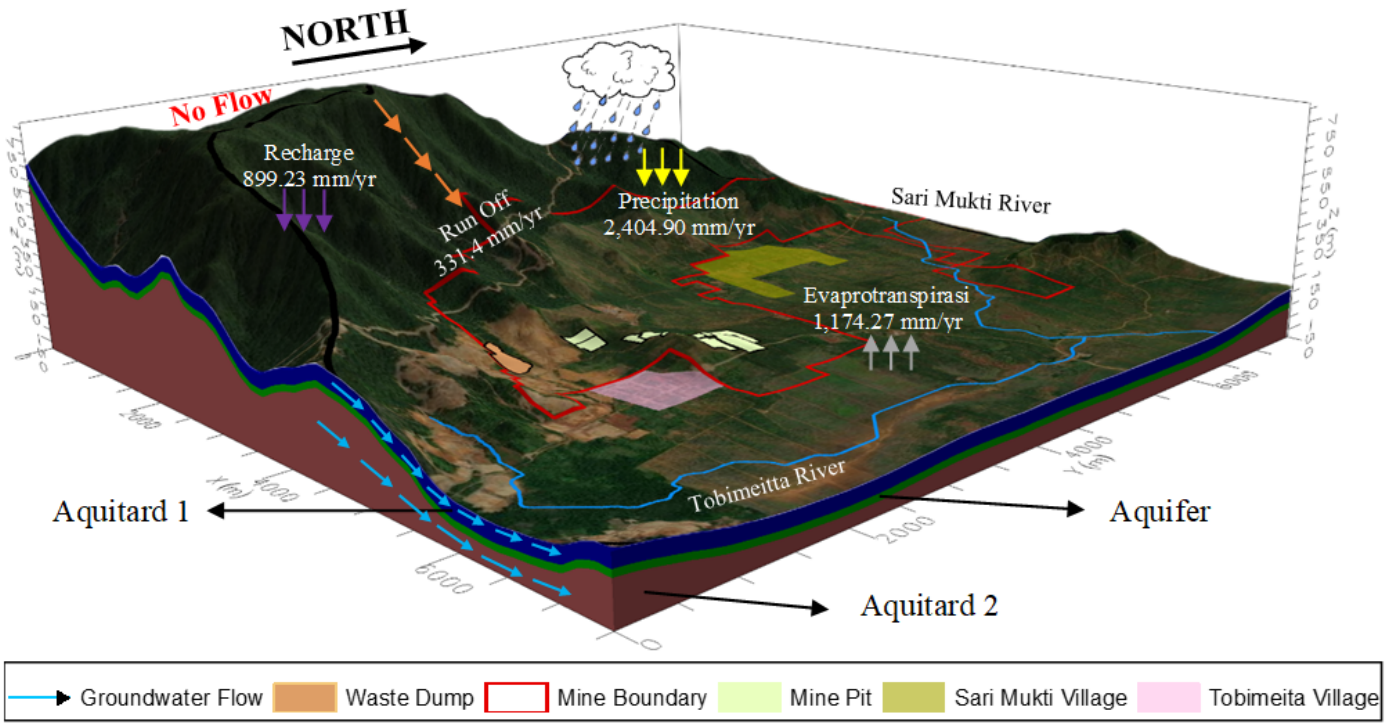

Figure 2

Groundwater Flow conceptual model

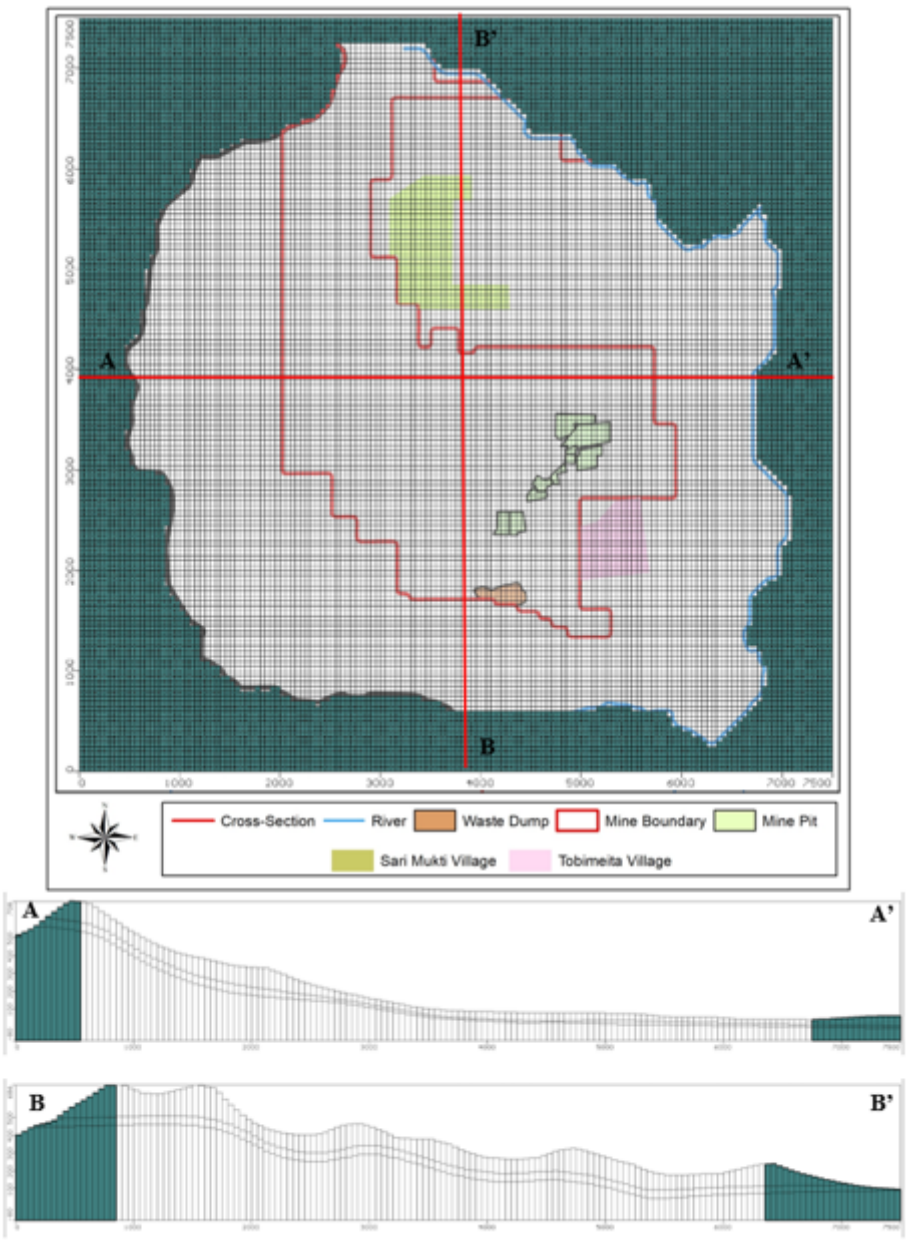

Figure 3

Discretization of the grid model

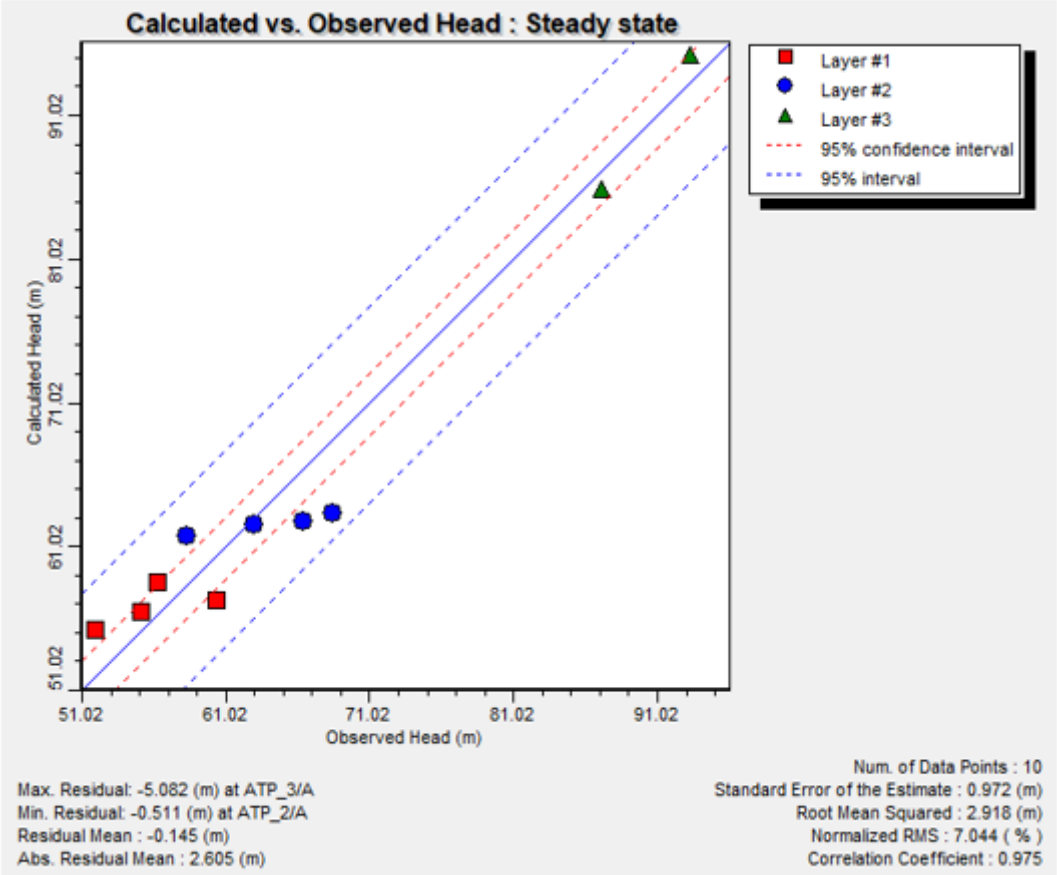

Figure 4

Scatter diagram of modeling results after calibration

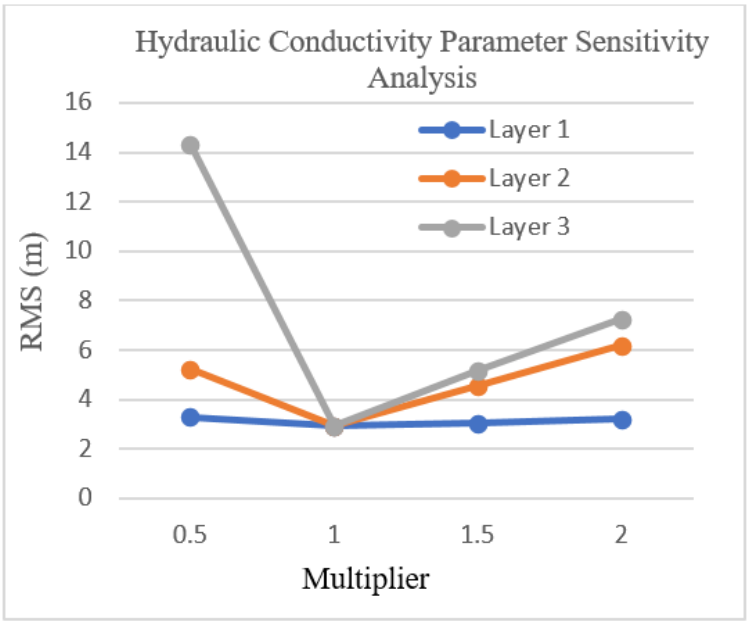

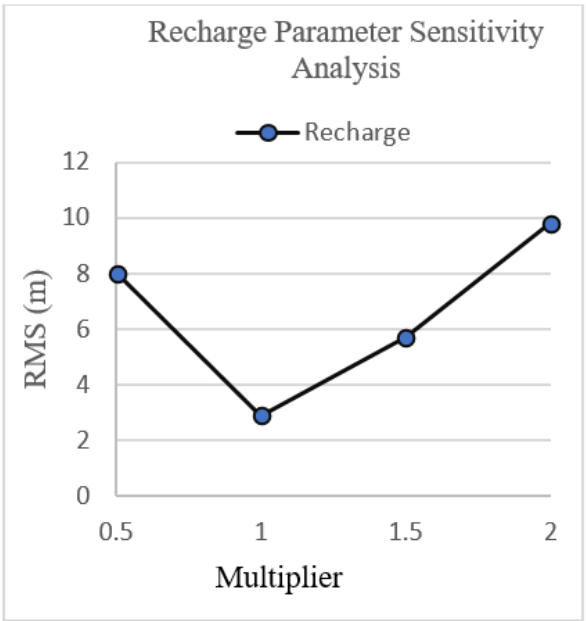

Figure 5

a) The sensitivity of the hydraulic conductivity parameter, b) the sensitivity of the recharge parameter.

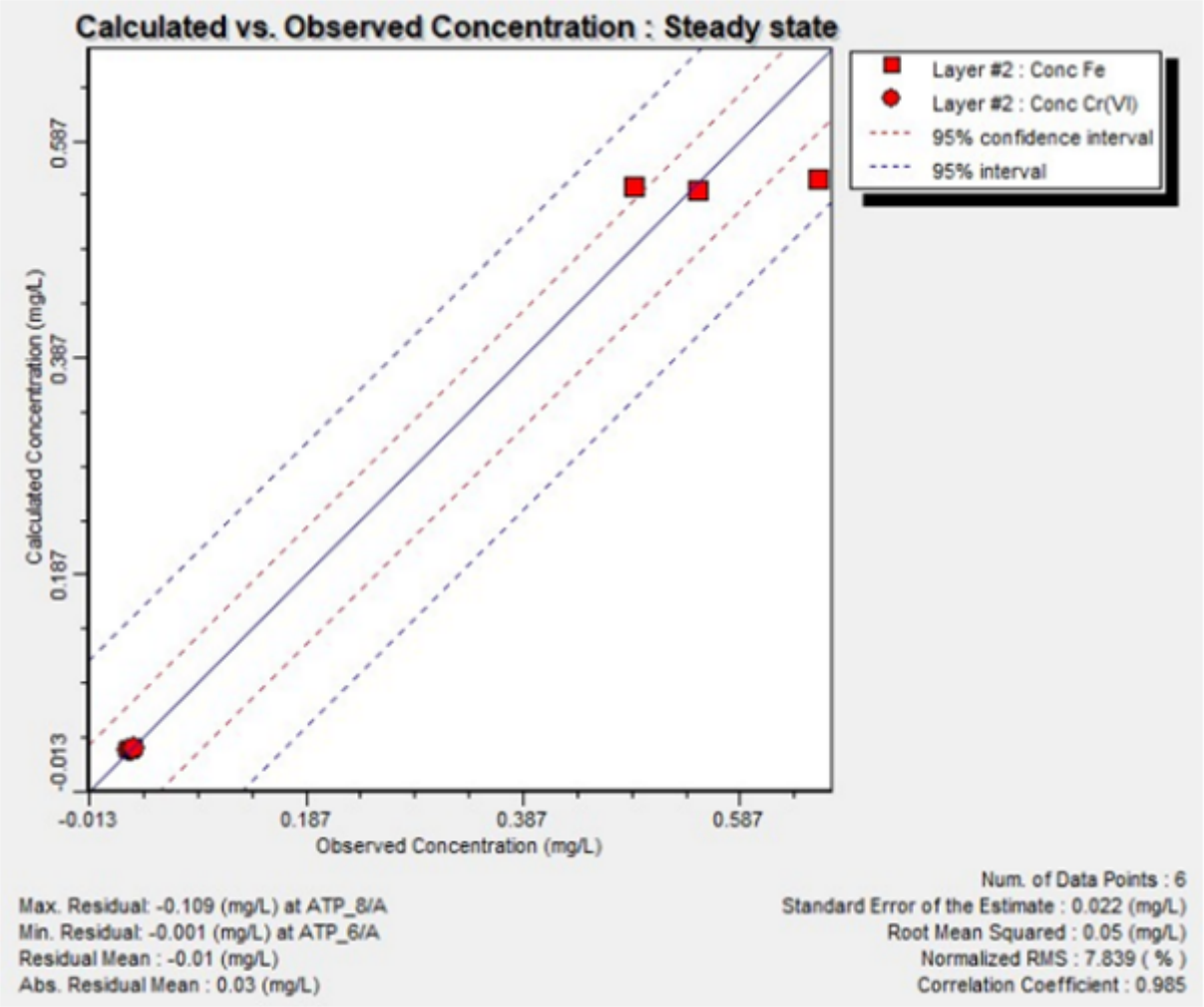

Figure 6

Scatter diagram of contaminant transport modeling results

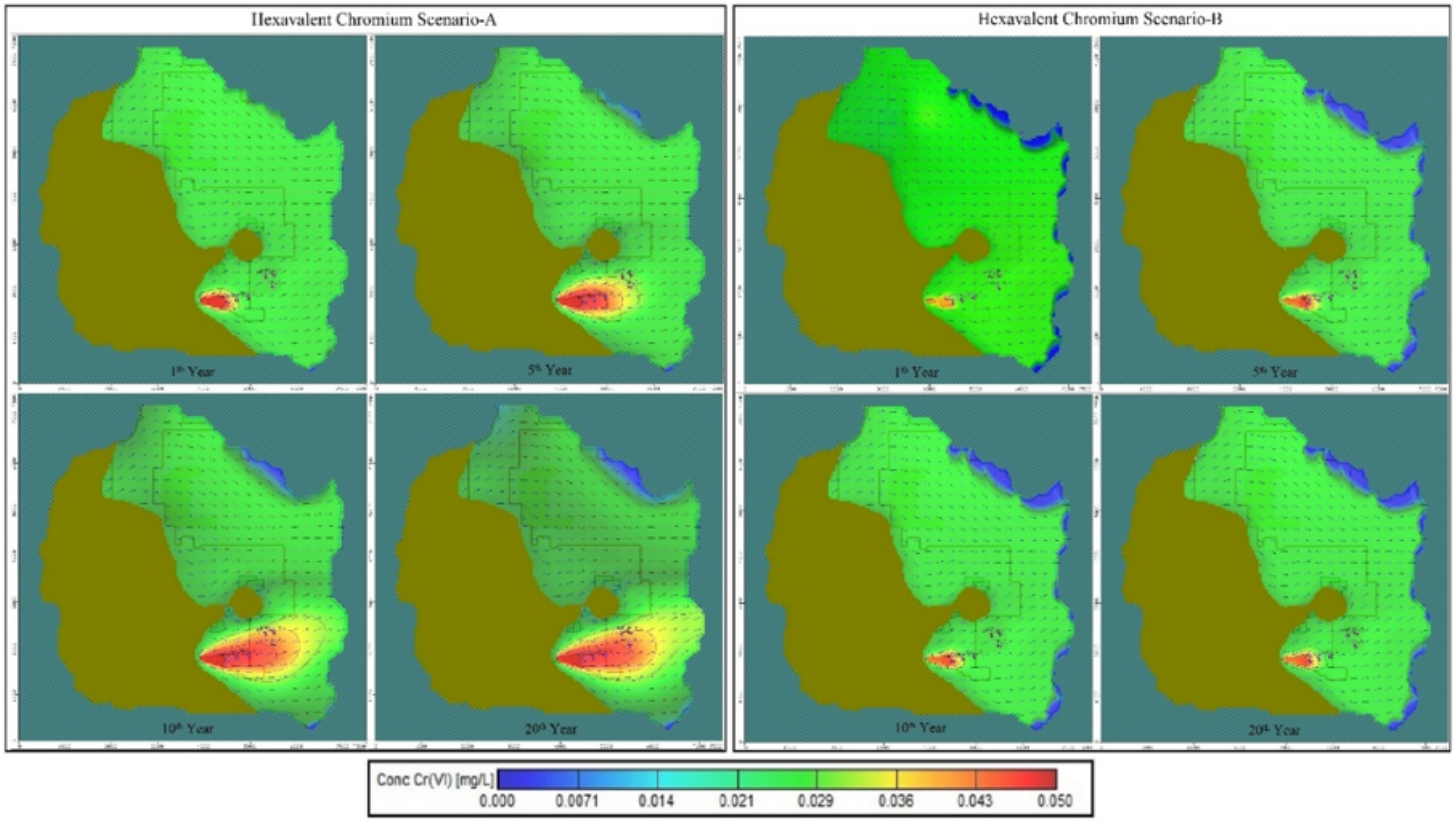

Figure 7

Simulation of hexavalent chromium contaminant transport (a) Scenario-A (b) Scenario-B

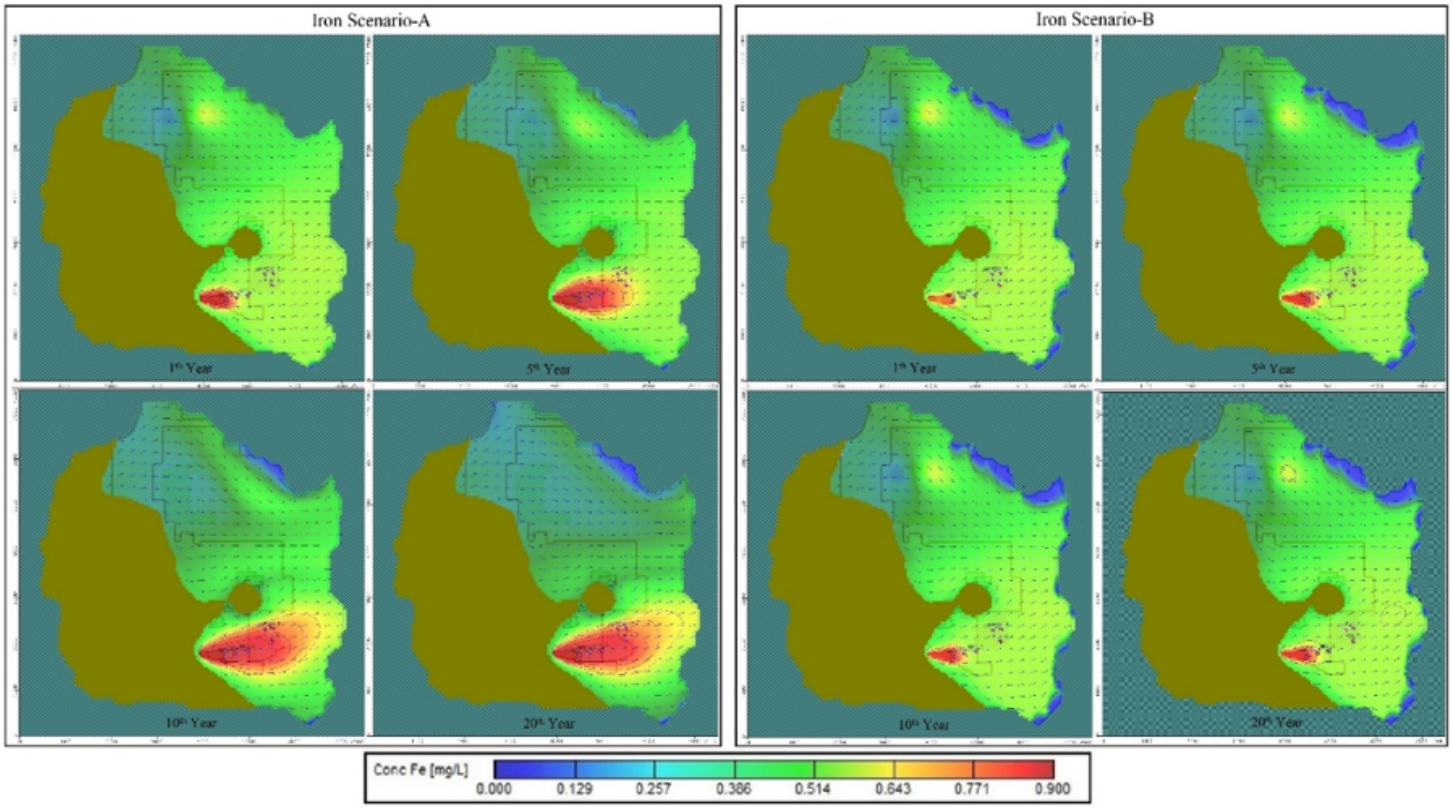

Figure 8

Simulated transport of iron contaminants (a) Scenario-A(b) Scenario-B